



## STRUCTURAL HEALTH MONITORING OF TORRE CENTRAL BY THE WAVE METHOD

M. Rahmani<sup>(1)</sup>, T.-Y. Hao<sup>(2)</sup>, M. Todorovska<sup>(3)</sup>, R. Boroschek<sup>(4)</sup>

<sup>(1)</sup> Research Associate, University of Southern California, Los Angeles, California, U.S.A., [mrahmani@usc.edu](mailto:mrahmani@usc.edu)

<sup>(2)</sup> Assistant Professor, California State University, Northridge, California, U.S.A., [tong-ying.hao@csun.edu](mailto:tong-ying.hao@csun.edu)

<sup>(3)</sup> Research Professor, University of Southern California, Los Angeles, California, U.S.A., [mtodorov@usc.edu](mailto:mtodorov@usc.edu)

<sup>(4)</sup> Professor, University of Chile, Santiago de Chile, CHILE, [rborosch@ing.uchile.cl](mailto:rborosch@ing.uchile.cl)

### Abstract

This paper presents preliminary structural health monitoring analysis of Torre Central, a 9-story reinforced concrete (RC) shear wall building in Santiago de Chile, by the wave method using recorded accelerations during 51 earthquakes over a period of two years (2009-2011). The set includes the M8.8 Maule earthquake of February 27, 2010. The building was 110 km from the rupture and was lightly damaged from this earthquake. The method is based on identifying the velocity of vertically propagating waves through the structure, which is related to the structural stiffness, and monitoring its changes. In this paper, the velocity is identified by fitting a 2-layer shear beam model in the observed response by matching, in the least squares sense, pulses in impulse responses. Only the EW response is analyzed. Two types of analysis are presented. The Maule earthquake response was analyzed in moving windows of lengths 10 s, 15 s and 20 s. The results show permanent drop in wave velocity ~20%. Additionally, all 51 events were analyzed in single time windows. Plots of the identified wave velocities vs. interstory drift show decreasing wave velocity with increasing drift and permanent change of ~11% in wave velocity at small strain level (peak drift  $\sim 10^{-6}$ ). The changes in wave velocity are in general agreement with published results on changes in the frequencies of vibration.

*Keywords: structural health monitoring; wave method; wave propagation in buildings; Maule, Chile earthquake of 2010*

### 1. Introduction

Torre Central is a 9-story reinforced concrete (RC) shear wall building on the campus of the University of Chile, in Santiago de Chile (Fig. 1). The building was permanently instrumented in 2009 with 8 seismic sensors (uniaxial accelerometers) and 17 environmental sensors (measuring wind speed and direction, temperature, rainfall, and ambient and soil humidity), and since then is being continuously monitored by a web based system [1, 2]. Numerous earthquakes as well as microtremors have been recorded and analyzed by modal methods [1]. This paper presents the first application of the wave method to this building.

This paper presents analysis of 51 earthquakes recorded in the building over a period of two years, between August of 2009 and September of 2011, including the great M8.8 Maule earthquake of February 27, 2010, which occurred south-west from the building, the closest distance from the rupture being ~110 km. The observed structural damage after the Maule earthquake has been characterized as low, consisting of minor cracks in the shear walls and non-structural elements. The objective of this paper is to estimate the velocity of vertically propagating waves through the structure and its variability over the observation period of two years, including dependence on the level of response and permanent changes caused by the Maule earthquake.

The wave method is a relatively recent method for SHM. It is based on the premise that change in structural stiffness, possibly caused by damage, would cause change in the velocity of wave propagation through the structure. In this study, the lateral deformation of the building as a whole is modeled by a shear beam with

piecewise constant properties along the height, i.e. a layered shear beam with the layers representing groups of floors between sensors [3, 4]. The beam shear wave velocity is identified by matching in the least squares sense pulses propagating vertically through the structure from a virtual source at the top. Such pulses are generated by deconvolution of the recorded response at different levels with the response at the top of the structure [5]. The identified beam velocity is the vertical phase velocity in the layers, which is equal to the shear wave velocity if the deformation is in pure shear. In this paper, only the EW (longitudinal) response was analyzed, for which the one dimensional (1D) model was found to be suitable. The records of the NS response were significantly affected by the torsional responses, due to asymmetry in the arrangement of the shear walls, for which a 1D model cannot account. A two-layer shear beam was fitted, one layer representing the part of the building between the 2<sup>nd</sup> basement and the 3<sup>rd</sup> floor and the other part between the 3<sup>rd</sup> and 8<sup>th</sup> floors.

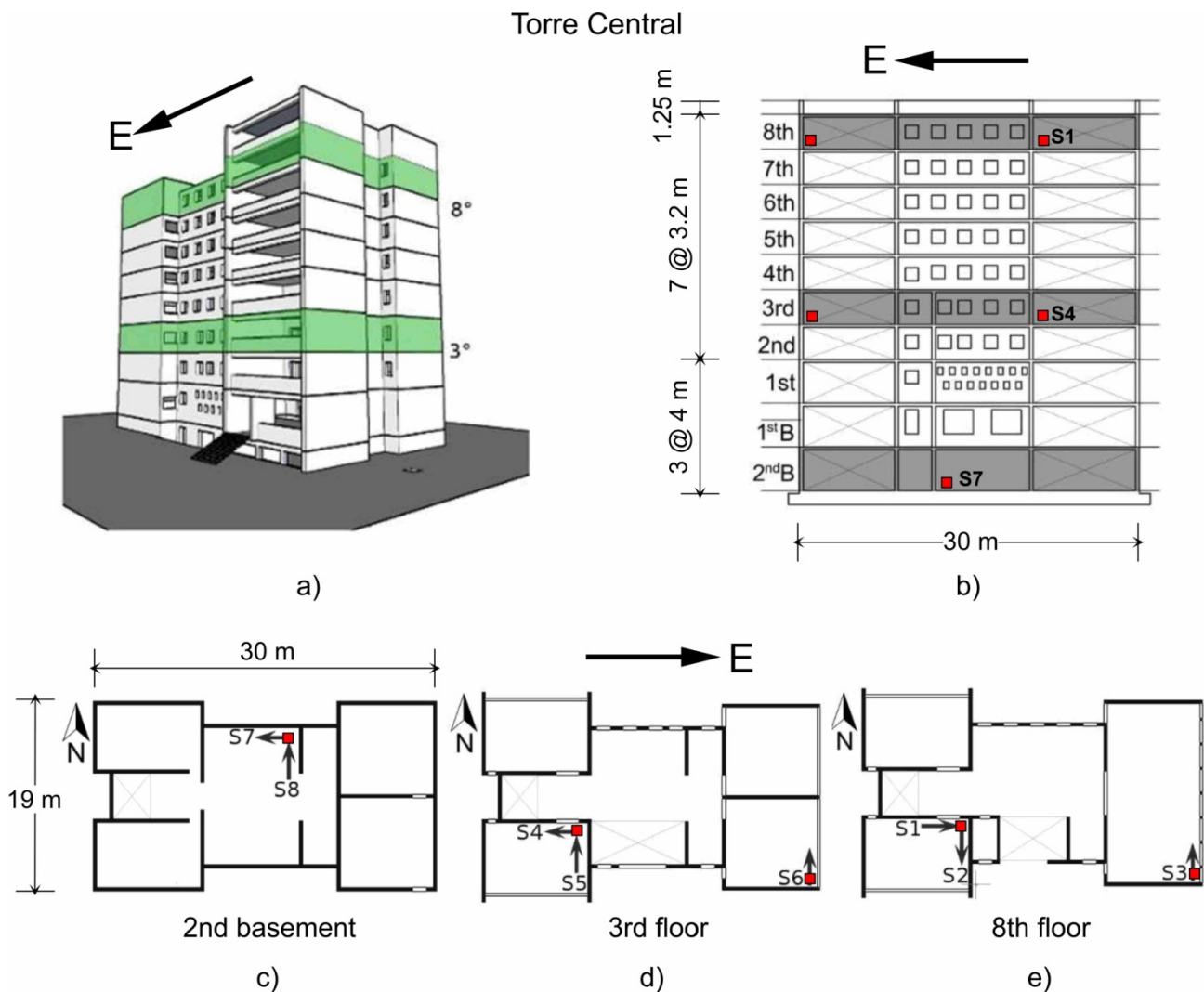


Fig. 1 – Torre Central building: a) Three dimensional sketch; b) EW elevation along the North side of the building; c), d) and e) 2<sup>nd</sup> basement, 3<sup>rd</sup> and 8<sup>th</sup> floor plans showing the sensor location and orientation (adapted from [1] with minor modifications).

## 2. Building Description and Strong Motion Data

Torre Central has nine-stories above ground and a two-level basement, with the 1st floor being at ground level. It is the home of the Faculty of Physical and Mathematical Science of University of Chile, Santiago de Chile. The building was constructed in 1962 with a floor footprint approximately 30 by 18 m and a height of 30.2 m. The lateral force resisting system consists of RC walls in both longitudinal and transverse directions, not symmetrically distributed in plan. The typical wall thickness is 35cm, and the typical slab thickness is 25 cm. The ratio of average wall-to-plan area above the basement is 7.7%. The foundation soil consists of dense gravel and corresponds to soil class C according to the ASCE7-10 code [1]. In the past decade, the building was structurally modified. E.g., several floors were remodeled, making new openings on the shear walls for doors and windows, while other openings were covered. In addition, a metal facade for air conditioner equipment on the exterior was installed [1]. Fig. 1 illustrates the perspective (part a)), the EW elevation along the North side of the building (part b)), and the plan views of the instrumented floors (parts c) through e)) (adapted from [1] with minor modifications).

The seismic monitoring system consists of 8 force balance accelerometers, with dynamic range of 135 db between 0.01 and 50 Hz and 145 db between 0.01 and 20 Hz, an analog to digital converter and a central recording system with 16 bit resolution. The system has two parallel data acquisition systems, one recording triggered events and the other one recording the amplified signal continuously [2]. The sensor location is shown by small squares in Fig. 1.

Fig. 2 shows a map of the location of the building and the epicenters of 40 of the 51 earthquakes analyzed in this study, which have been identified. The 51 events analyzed occurred between August of 2009 and September of 2011, of which 21 occurred before and 29 occurred after the M8.8 Maule earthquake of February 27, 2010. Of the smaller events, 40 have magnitude between 3.3 and 6.3, and 11 have unknown magnitude. The set represents a variety of levels of response, with peak average interstory drift ranging from  $10^{-7}$  to  $1.4 \times 10^{-3}$  for the EW response (Table A1).

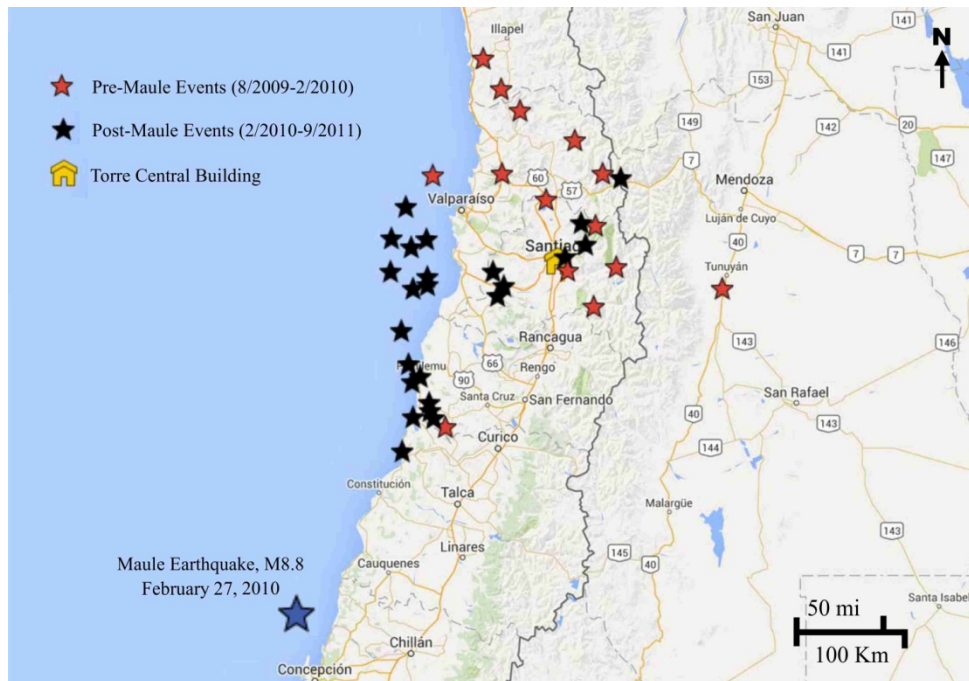


Fig. 2 – Google map showing the location of Torre Central and the epicenters of 51 earthquakes analyzed in this study (maps.google.com).

### 3. Methodology

The Maule earthquake was analyzed by the *time-velocity* algorithm [3], which is an extension to moving window analysis of the *waveform inversion* algorithm for identification of buildings, introduced by Rahmani and Todorovska [4]. In each time window, the vertical wave velocity of the building is identified by fitting an equivalent layered shear beam model in the recorded acceleration response. This is done by matching, in the least squares (LSQ) sense, the main lobes of the acausal and causal propagating pulses in the deconvolved responses by the response at the roof. The deconvolved responses represent the building impulse response functions (IRF), i.e. the responses at the instrumented levels to a virtual source located at the roof. The pulses are fitted simultaneously at all levels where motion was recorded. The identified vertical wave velocities of the layers are mapped on time-velocity graphs, which depict their temporal variation during the earthquake shaking. Inference on loss of stiffness, possibly due to damage, is made based on the changes in the identified velocities relative to the values in the initial time window of smaller response, assuming that it represents the response of the undamaged structure [6, 7]. In the next section, the interferometric identification in a particular time window is reviewed, followed by a more detailed description of how the time-velocity graphs are constructed.

#### 3.1 Interferometric System Identification from Impulse Response Functions

Let  $u(z;t)$  be the response of the building at level  $z$  (measured downwards from the roof), and let  $\hat{u}(z, t_c, w_{win}; \omega)$  be its Fourier transform over a time window of width  $w_{win}$  and centered at  $t = t_c$  [3]. Further, let

$$\hat{h}(z, 0, t_c, w_{win}; \omega) = \frac{\hat{u}(z, t_c, w_{win}; \omega)}{\hat{u}(0, t_c, w_{win}; \omega)} \quad (1)$$

be the Transfer Functions (TF) between the windowed motions at level  $z$  and at the roof ( $z=0$ ) and let  $h(z, 0, t_c, w_{win}, \omega_{max}; t)$  be the corresponding Impulse Response Function (IRF), low-pass filtered in the band  $\omega \in (0, \omega_{max})$

$$h(z, 0, t_c, w_{win}, \omega_{max}; t) = \frac{1}{2\pi} \int_{-\omega_{max}}^{\omega_{max}} \hat{h}(z, 0, t_c, w_{win}; \omega) e^{-i\omega t} d\omega \quad (2)$$

To avoid division by very small numbers in Eq. (1), regularized TFs are computed [7]

$$\hat{h}(z, 0, t_c, w_{win}; \omega) = \frac{\hat{u}(z, t_c, w_{win}; \omega) \overline{\hat{u}(0, t_c, w_{win}; \omega)}}{|\hat{u}(0, t_c, w_{win}; \omega)|^2 + \varepsilon} \quad (3)$$

where the bar indicates complex conjugate and  $\varepsilon$  is a regularization parameter (in this paper,  $\varepsilon = 0.1\%$  of the average power of the reference signal).

As known from linear systems theory, the IRF is a representation of the systems function in the time domain, and it represents the response of the system to a virtual pulse applied at the reference level [9]. The IRF at the reference level gives the virtual pulse, which is a *sinc* function when  $\omega_{max} < \infty$  [3]. The observed IRFs are computed from recorded accelerations.

The model that is fitted is an elastic, viscously damped, shear beam, with piecewise uniform material properties, excited by vertically incident shear waves [6, 7]. The layers are characterized by thickness  $h_i$ , mass density  $\rho_i$ , and shear modulus  $\mu_i$ , which gives shear wave velocities  $v_i = \sqrt{\mu_i / \rho_i}$  and quality factor  $Q(f)$  (the damping ratio  $\zeta = 1/(2Q)$ ). In this paper, the layers comprise of the part of the building between the instrumented floors. Layering is introduced to enable finding the spatial distribution of the severity of damage. Perfect bond of the layers is assumed. The layers move *only* horizontally. For this generic model, both TFs and

low-pass filtered IRFs can be computed analytically, from the propagator of the medium [10], by simple recursive equations [8, 11].

The model IRFs are fitted to the observed IRFs over selected time windows with length  $w_{pulse}$ , chosen to contain the acausal and causal pulses. It is assumed that, within each time window, the system is linear and the transient response (due to nonzero initial conditions) can be neglected, and that the results of the fit would be robust to violation of these assumptions [12]. More details about the moving window analysis algorithm can be found in [3].

The methodology is illustrated in Fig. 3 on a real example for this building, which is the recorded response of the earthquake of 2/12/2010 (M=6, R=151 km). Part a) shows the model fitted, which is a 2-layer shear beam, with assumed mass density  $\rho_1 = \rho_2 = 300 \text{ kg/m}^3$  and assumed piecewise constant damping ratio,  $\zeta = 2\%$  for  $f \leq 4 \text{ Hz}$  and  $\zeta = 5\%$  for  $f > 4 \text{ Hz}$ . Part b) shows the agreement of the observed and fitted model impulse responses on the band of the fit,  $1.2 < f < 8.5 \text{ Hz}$ , and part c) shows the observed transfer-function, meant to illustrate the frequency content in the response. It can be seen from part c) that the transfer-function of the EW response resembles that of shear beam except for a relatively small coupling effect with the NS response at  $\sim 2 \text{ Hz}$ .

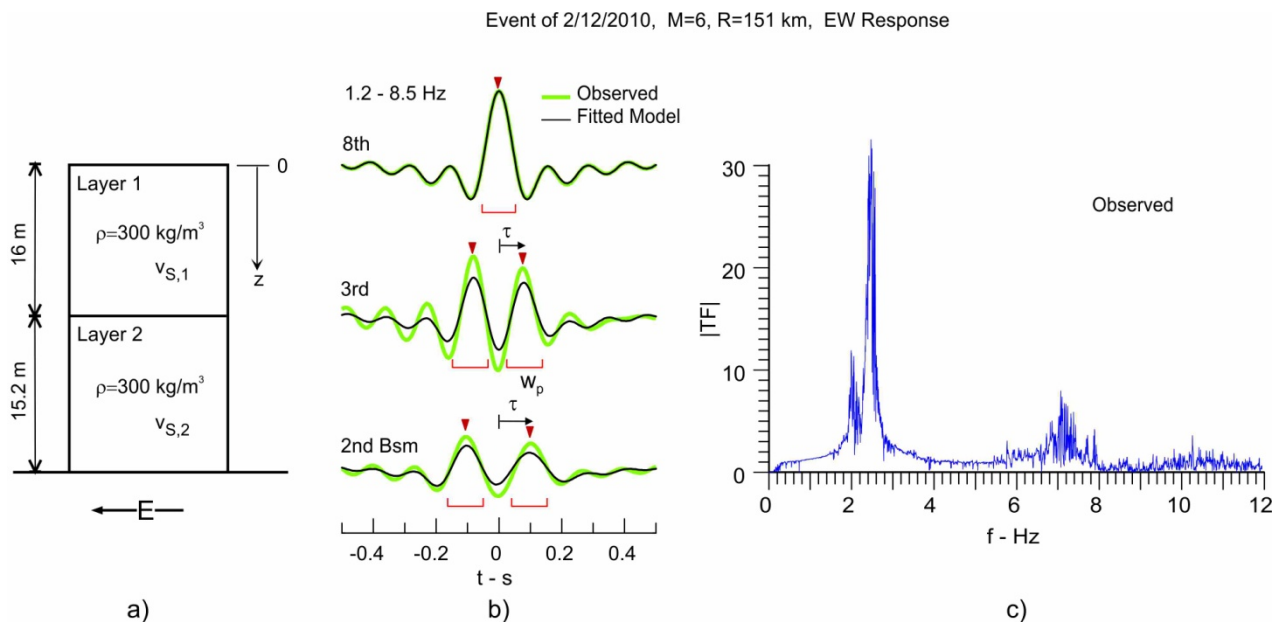


Fig. 3 – Illustration of the LSQ fit: a) the fitted model, and b) observed and fitted Impulse Responses. The EW response of the event of 2/12/2010, M=6, R= 151 km is used as an example. As background information, part c) shows the observed transfer function between 8th floor and 2nd basement responses.

#### 4. Results and Analysis

The analysis consists of two parts. The first part consists of moving window analysis of the Maule earthquake and the second part consists of the single window analysis of all 51 events.

### 4.1 Time-Velocity Analysis of the Maule Earthquake

Fig. 4 shows the recorded EW accelerations (part a)), their Fourier Transform amplitudes (part b)), and the transfer-function between the responses on the 8<sup>th</sup> floor and 2<sup>nd</sup> basement (part c)), shown to illustrate the bandwidth of the transfer-function. At the 8<sup>th</sup> floor, the peak acceleration was  $442.5 \text{ cm/s}^2$  (Table A1).

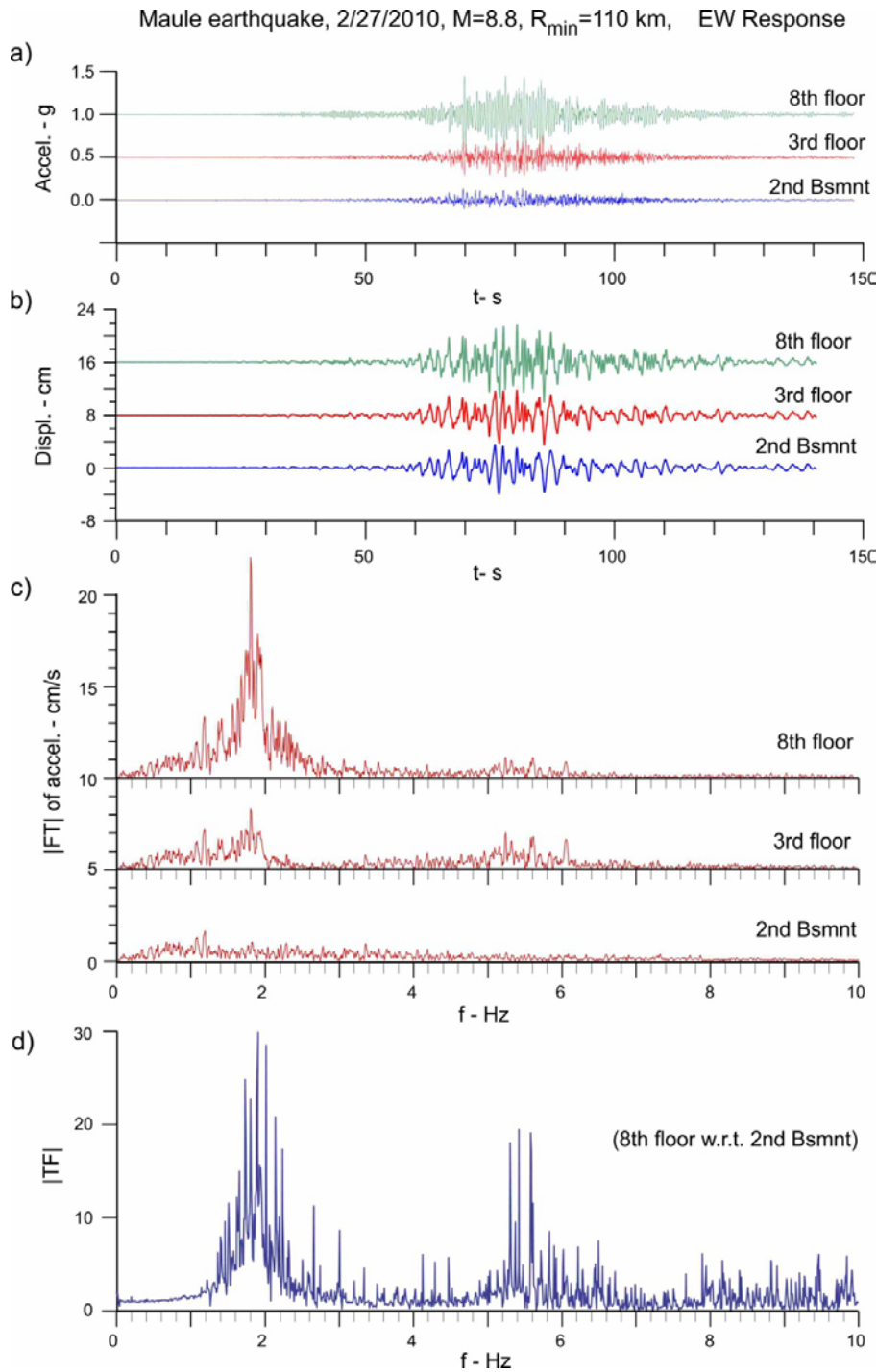


Fig. 4 – EW response of Torre Central to the Maule, 2010, earthquake. Acceleration time histories and Fourier transform amplitudes (parts a) and b)), and Transfer-Function between responses at 8<sup>th</sup> floor and 2<sup>nd</sup> basement (part c)).

Fig. 5 shows the results of the time velocity analysis based on a fitted 2-layer model. The different symbols show the layer velocity measured for different widths of the moving time window vs. the central time of the window. The layer drift is shown at the bottom to illustrate the level of deformation. It can be seen that the peak layers drifts (~0.14% in the upper part and ~0.08% in the lower part) were well below the *Immediate Occupancy* performance level (0.5% peak transient drift for concrete shear wall) set by ASCE/SEI 41 Standard [13]. Fig. 6 illustrates the observed impulse responses and transfer functions in two of the moving windows, one at the beginning and the other one at the end of shaking. Permanent time shift of the propagating pulses as well as frequency shift of the modal frequencies can be seen suggesting permanent change of stiffness. Fig. 5 suggests permanent change in layers 1 and 2 velocities roughly of ~22% and ~19%.

Fig. 7 shows results of time velocity analysis for fitted equivalent uniform shear beam. The equivalent uniform beam velocity was computed from the layer velocities based on the *ray theory* assumption that the travel time through both layers is the sum of the travel times through the individual layers

$$\frac{h_1 + h_2}{v_{eq}} = \frac{h_1}{v_{s,1}} + \frac{h_2}{v_{s,2}} \quad (4)$$

This figure shows considerably less scatter and permanent change of  $v_{eq}$  of ~20%.

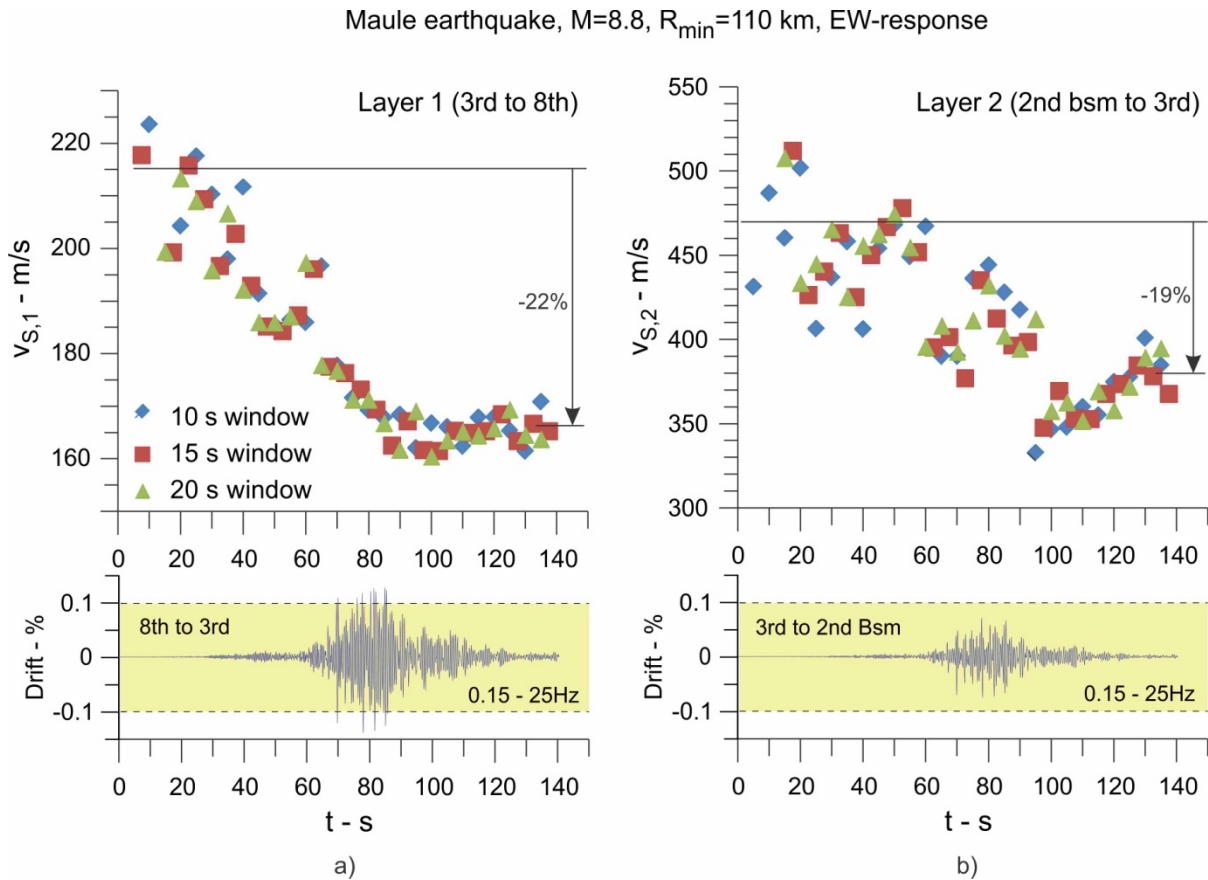


Fig. 5 – Time-velocity analysis of the Maule earthquake EW response, based on fitted 2-layer shear beam model: (a) Layer 1 (2<sup>nd</sup> basement to 3<sup>rd</sup> floor) and (b) Layer 2 (4<sup>th</sup> to 8<sup>th</sup> floors). Results are shown for three widths of the moving window,  $w_{win} = 10, 15$  and  $20$  s, all shifted by 5 s. The Impulse responses were fitted on the band 0 - 8 Hz. The layer drift is shown on the bottom (0.15 - 25 Hz).

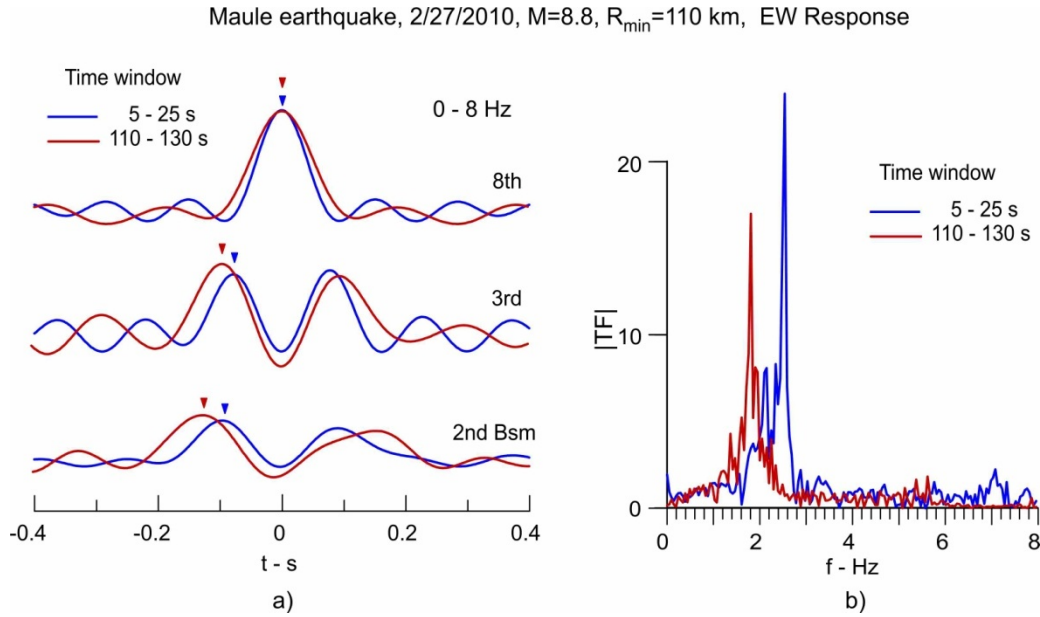


Fig. 6 – Comparison of observed system functions in two of the moving windows in Fig. 5, one early (5-25 s) and the other one late (110-130 s): a) Impulse Responses and b) Transfer-Functions

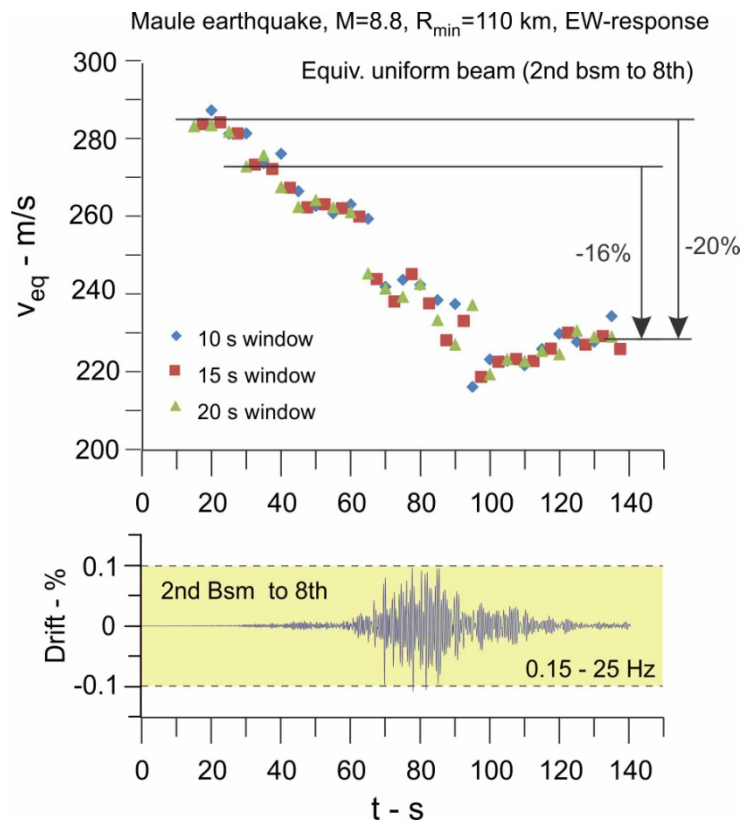


Fig. 7 – Time-velocity analysis of the Maule earthquake EW response, based on fitted equivalent uniform shear beam model (2<sup>nd</sup> basement to 8<sup>th</sup> floor). Results are shown for three widths of the moving window,  $w_{win} = 10, 15$  and  $20$  s, all shifted by  $5$  s. The Impulse responses were fitted on the band  $0-8$  Hz. The layer drift is shown on the bottom.

## 4.2 Wave Velocities during 51 Events

Fig. 8 shows the layer velocities and the equivalent uniform beam velocity plotted vs. peak drift, measured in single time window for all 51 events (Fig. 2). Different symbols are used to differentiate between the events before and after the Maule earthquake. It can be seen that the two sets of points represent two different populations, each represented by its own variation of wave velocity with peak drift. The shift between populations suggests permanent change in stiffness due to damage caused by Maule earthquake. At small strain level (peak drift  $\sim 10^{-6}$ ), the permanent change in the equivalent wave velocity is  $\sim 11\%$ .

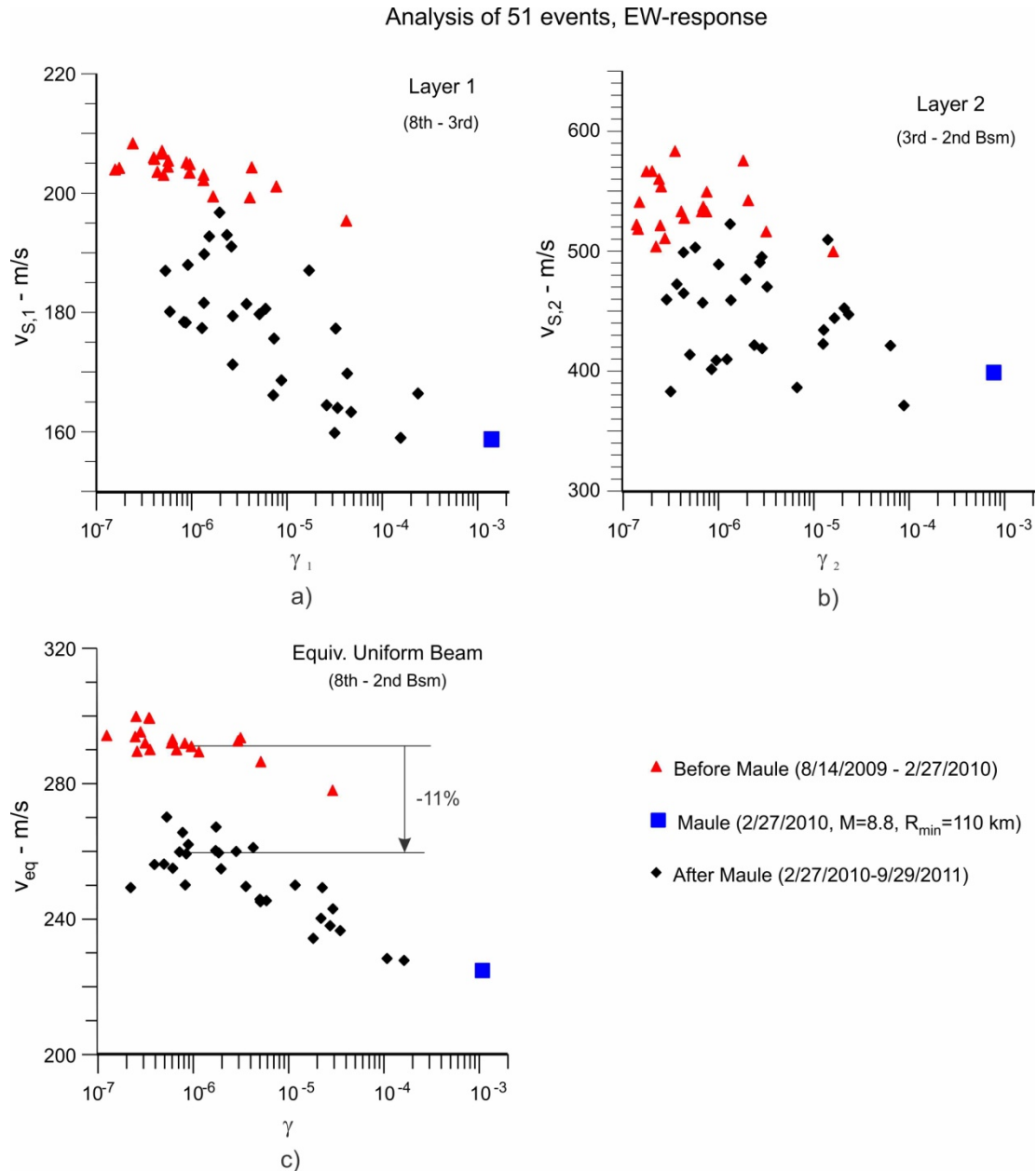


Fig. 8 – Identified vertical wave velocities from recorded EW response during 51 events (see Fig. 2) vs. peak interstory drift,  $\gamma$ . a) Layer 1; b) Layer 2; c) Equivalent uniform beam. The Impulse responses were fitted on the band 1.2 - 8 Hz, and the peak drift was computed on the band 0.15 – 25 Hz.

## 5. Conclusions

Both the moving window analysis of the Maule, 2010 earthquake and the single window analysis of the 50 smaller events suggest that permanent loss of stiffness occurred in the EW stiffness of the building. The change was comparable in the top and bottom part of the building. At smaller strain levels (peak drift  $\sim 10^{-6}$ ), the change in velocity is  $\sim 11\%$ , and at larger strain levels it is about 20%. These changes are comparable with those detected in the frequencies of vibration [1, 2].

## 6. References

- [1] Boroschek RL, Carreno RP (2011): Period variations in a shear wall building due to earthquake shaking, *5th International Conference on Structural Health Monitoring of Intelligent Infrastructure (SHMII-5)*, 11-15 December 2011, Cancún, México.
- [2] Boroschek R, Tamayo F, Aguilar RL (2014): Evaluation of the environmental effects on a medium rise building, *7th European Workshop on Structural Health Monitoring*, July 8-11, 2014. La Cité, Nantes, France.
- [3] Rahmani M, Ebrahimian M, Todorovska MI (2015): Time-wave velocity analysis for early earthquake damage detection in buildings: Application to a damaged full-scale RC building, *Earthq. Eng. Struct. Dyn.*, Special issue on: *Earthquake Engineering Applications of Structural Health Monitoring*, CR Farrar and JL Beck Guest Editors, **44** (4), 619–636, doi: 10.1002/eqe.2539.
- [4] Rahmani MT, Todorovska MI (2013): 1D system identification of buildings from earthquake response by seismic interferometry with waveform inversion of impulse responses – method and application to Millikan Library, *Soil Dynamics and Earthquake Engng*, Jose Manuel Roësset Special Issue, E. Kausel and J. E. Luco, Guest Editors, **47**, 157-174, doi: 10.1016/j.soildyn.2012.09.014.
- [5] Snieder R, Şafak E (2006): Extracting the building response using interferometry: theory and applications to the Millikan Library in Pasadena, California, *Bull. Seism. Soc. Am.*; **96** (2), 586-598.
- [6] Todorovska MI, Trifunac MD (2008): Earthquake damage detection in the Imperial County Services Building III: analysis of wave travel times via impulse response functions, *Soil Dynamics and Earthquake Engng*, **28** (5), 387–404, doi:10.1016/j.soildyn.2007.07.001.
- [7] Todorovska MI, Trifunac MD (2008): Impulse response analysis of the Van Nuys 7-story hotel during 11 earthquakes and earthquake damage detection, *Structural Control and Health Monitoring*, **15** (1), 90-116; doi: 10.1002/stc.208.
- [8] Todorovska MI, Rahmani MT (2013): System identification of buildings by wave travel time analysis and layered shear beam models - spatial resolution and accuracy, *Structural Control and Health Monitoring*, **20** (5), 686–702, doi: 10.1002/stc.1484.
- [9] Oppenheim AV, Schaffer RW, Buck JR (1999): *Discrete-Time Signal Processing*, Prentice Hall; 2 edition, Upper Saddle River, New Jersey.
- [10] Gilbert F, Backus GE (1966): Propagator matrices in elastic wave and vibration problems, *Geophysics*, **XXXI** (2), 326-332.
- [11] Trampert J, Cara M, Frogneux M (1993). SH propagator matrix and  $Q_S$  estimates from borehole- and surface-recorded earthquake data, *Geophys. J. Int.*, **112**, 290-299.
- [12] McVerry GH (1979): Frequency domain identification of structural models from earthquake records, *Report No. EERL 79-02*, Earthquake Engineering Research Laboratory, California Institute of Technology, Pasadena, CA.
- [13] American Society of Civil Engineers (ASCE) (2007): Seismic rehabilitation of existing buildings, *Report ASCE/SEI 41-06*, American Society of Civil Engineers, Reston, Virginia.

## Appendix: List of Events Analyzed and Identified Wave Velocities

Table A1 - List of the 51 earthquakes analyzed. The earthquakes date, magnitude, epicentral distance R, and the peak roof acceleration (PRA) are shown, as well as the peak layer drifts,  $\gamma$ , the identified wave velocities, V, and the frequency band on which the pulses in impulse responses were fitted.

EQ date	M	R [km]	PRA [cm/s <sup>2</sup> ]	V <sub>s,1</sub> [m/s]	$\gamma_1$ 10 <sup>-5</sup>	V <sub>s,2</sub> [m/s]	$\gamma_2$ 10 <sup>-5</sup>	V <sub>eq</sub> [m/s]	$\gamma$ 10 <sup>-5</sup>	f [Hz]
08/05/2009 (14:12)	3.7	141.7	-0.46	206.6	0.04800	566.9	0.02000	299.2	0.03423	1.2 - 8
08/05/2009 (21:20)	-	-	0.54	205.2	0.08631	533.5	0.04040	293.0	0.06035	1.2 - 8
08/14/2009 (13:46)	3.6	46.3	-1.37	204.9	0.09400	527.9	0.04349	291.9	0.05901	1.2 - 8
08/14/2009 (22:00)	-	-	5.84	201.1	0.76244	516.8	0.31388	286.3	0.50961	1.2 - 7.8
08/18/2009	-	-	0.45	207.1	0.04794	566.8	0.01743	299.7	0.02506	1.2 - 8
08/23/2009	-	-	-0.67	204.4	0.05525	583.8	0.03480	299.1	0.03478	1.2 - 8
11/20/2009	4.5	180.6	1.28	199.5	0.16512	549.9	0.07487	289.2	0.11414	1.2 - 7.8
11/24/2009	4.4	197.4	0.62	203.6	0.04294	560.4	0.02368	295.1	0.02792	1.2 - 8
11/27/2009	-	-	-0.28	208.3	0.02369	518.8	0.01428	294.0	0.01234	1.2 - 8
12/13/2009	3	12.4	-0.45	204.2	0.01706	541.3	0.01474	293.1	0.00949	1.2 - 8
12/17/2009	3.6	137.9	0.49	205.8	0.04000	521.8	0.02434	291.8	0.03128	1.2 - 8
12/20/2009	3.6	88.8	0.55	206.0	0.03919	504.2	0.02204	289.4	0.02567	1.2 - 8
12/27/2009	4.6	165.6	-1.50	203.1	0.13088	533.4	0.07421	290.8	0.09538	1.2 - 8
12/28/2009	3.3	12.8	1.12	203.1	0.04975	554.1	0.02493	293.7	0.02452	1.2 - 8
01/01/2010 (09:17)	3.9	52.7	-0.48	205.5	0.05581	511.1	0.02730	289.9	0.03516	1.2 - 8
01/01/2010 (14:53)	4.1	53.0	1.16	203.4	0.09356	537.6	0.06881	291.8	0.08141	1.2 - 8
01/13/2010	3.3	94.7	-0.29	204.0	0.01544	522.5	0.01375	290.1	0.00897	1.2 - 8
01/18/2010	-	-	2.85	204.3	0.42050	542.6	0.20329	293.4	0.31337	1.2 - 8
01/19/2010	5	110.9	-3.10	199.3	0.40256	575.7	0.18000	292.4	0.29372	1.2 - 8
02/05/2010	3.9	56.3	-2.20	202.2	0.13062	533.4	0.06638	289.8	0.06673	1.2 - 8
02/12/2010	6	150.8	22.02	195.4	4.14895	500.1	1.57507	277.9	2.88779	1.2 - 8
2/27/2010 Maule	8.8	110*	442.5	158.8	139.68160	399.3	75.33701	224.7	108.11590	1.2 - 6.5
02/27/2010 (5:13)	5.6	133.9	18.73	164.1	3.35444	452.9	2.05539	238.0	2.72106	1.2 - 8
02/27/2010 (7:05)	4.8	119.7	3.05	166.2	0.70794	495.6	0.28184	245.7	0.50026	1.2 - 8
02/27/2010 (7:18)	-	-	3.17	175.7	0.72231	419.5	0.28388	245.0	0.50462	1.2 - 8
02/27/2010 (7:30)	6.1	121.5	-47.27	159.1	15.47425	421.7	6.26434	228.3	10.77561	1.2 - 7

EQ date	M	R [km]	PRA [cm/s <sup>2</sup> ]	V <sub>s,1</sub> [m/s]	$\gamma_1$ 10 <sup>-5</sup>	V <sub>s,2</sub> [m/s]	$\gamma_2$ 10 <sup>-5</sup>	V <sub>eq</sub> [m/s]	$\gamma$ 10 <sup>-5</sup>	f [Hz]
02/27/2010 (16:00)	5.9	152.5	-31.02	163.4	4.65413	447.6	2.27993	236.5	3.47888	1.2 - 7.5
02/27/2010 (20:13)	-	-	-14.82	169.8	4.25056	444.7	1.62494	243.0	2.90753	1.2 - 8
03/01/2010	4.2	147.1	1.22	177.4	0.12619	503.4	0.05671	259.2	0.08426	1.2 - 7.5
03/02/2010	-	-	-0.60	178.4	0.08550	465.3	0.04290	254.9	0.06080	1.2 - 8
03/03/2010	-	-	12.36	159.9	3.12775	509.9	1.38264	240.2	2.18724	1.2 - 8
03/04/2010	3.6	120.2	-0.40	180.2	0.05800	460.0	0.02842	256.0	0.03907	1.2 - 8
03/11/2010 (11:39)	6.3	164.6	-117.4	166.5	23.51213	371.9	8.66184	227.7	16.24535	1.2 - 7
03/11/2010 (12:06)	5.9	171.7	15.11	164.5	2.58063	423.1	1.23717	234.2	1.81231	1.2 - 8
03/11/2010 (13:23)	5.3	163.2	6.00	168.7	0.86412	470.7	0.32046	245.4	0.58513	1.2 - 8
03/11/2010 (23:36)	-	-	0.76	181.6	0.13231	414.2	0.04980	250.0	0.08228	1.2 - 8
03/27/2010 (02:57)	3.3	63.7	0.94	187.0	0.05213	383.5	0.03138	249.2	0.02199	1.2 - 8
03/27/2010 (16:39)	4.1	59.6	2.53	171.3	0.26450	523.0	0.13151	254.8	0.19551	1.2 - 7.5
04/07/2010	4.9	177.8	3.28	179.8	0.50694	422.2	0.23474	249.5	0.35564	1.2 - 8
05/21/2010	5.5	173.2	-12.49	177.4	3.21275	434.8	1.25092	249.2	2.25289	1.2 - 8
05/26/2010	3.8	54.4	-1.36	189.8	0.13300	457.3	0.06770	265.4	0.07715	1.2 - 7.5
06/11/2010	5.1	192.3	1.57	193.0	0.23119	410.3	0.12151	260.1	0.17138	1.2 - 8
06/22/2010	4.7	180.8	1.65	191.1	0.25688	459.6	0.13388	267.1	0.17320	1.2 - 8
08/15/2010	4.3	40.0	-2.41	192.8	0.15056	409.5	0.09408	259.7	0.07157	1.2 - 8
05/22/2011	3.6	7.1	-0.99	178.5	0.08144	472.9	0.03632	256.1	0.04923	1.2 - 8
06/05/2011	5.6	221.5	7.51	187.1	1.68400	386.8	0.65842	249.9	1.17138	1.2 - 8
06/08/2011	4.9	155.7	-2.03	181.5	0.37000	477.0	0.19204	259.9	0.28116	1.2 - 8
07/28/2011	3.7	94.2	-0.60	188.0	0.08975	499.3	0.04263	270.0	0.05256	1.2 - 8
08/26/2011	3.6	29.2	2.50	196.8	0.19300	402.1	0.08395	261.9	0.08856	1.2 - 8
08/28/2011	5.1	152.9	-3.50	180.7	0.58712	491.0	0.26934	261.0	0.42404	1.2 - 8
09/29/2011	4.2	134.1	1.59	179.4	0.26593	489.3	0.09954	259.5	0.18452	1.2 - 8

\* Closest distance from the rupture